Thioether complexes of $WSCl_4$, $WOCl_4$ and $WSCl_3$ and evaluation of thiochloride complexes as CVD precursors for WS_2 thin films

Danielle E. Smith[a], Victoria K. Greenacre[a], Andrew L. Hector[a], Ruomeng Huang[b], William Levason[a], Gillian Reid[a]*, Fred Robinson[a] and Shibin Thomas[a]

[a] School of Chemistry, University of Southampton, Southampton SO17 1BJ, UK; email: G.Reid@soton.ac.uk

[b] School of Electronics and Computer Science, University of Southampton, Southampton SO17 1BJ, UK

Abstract

The red-brown $[(WSCl_4)_2\{\mu\text{-}RS\{CH_2)_2SR\}]$ (R = Me, Ph, ^iPr) and $[(WSCl_4)_2\{\mu\text{-}MeS\{CH_2)_3SMe\}]$ have been made by reaction of $WSCl_4$ with the thioether in a 2:1 molar ratio, in anhydrous CH_2Cl_2 solution, and characterised by microanalysis, IR, UV/Vis and ^1H NMR spectroscopy. The X-ray structures of the four dithioether complexes reveal square pyramidal $WSCl_4$ units and bridging dithioethers with W=S *trans* to thioether sulfur. Paramagnetic W(V) complexes, $[WSCl_3\{RS\{CH_2)_2SR\}]$ (R = Me, ^iPr), have been made similarly using a 1: ≥1 ratio of reactants or longer reaction times. The W(VI) complexes, $[WSCl_4(SMe_2)]$ and $[WSCl_4(SeMe_2)]$, are also described. Analogous complexes of $WOCl_4$, $[(WOCl_4)_2\{RS(CH_2)_2SR\}]$ (R = Ph, ^iPr), have been made similarly from $WOCl_4$, but reactions using $MeS(CH_2)_nSMe$ (n = 2, 3) led to reduction to W(V), forming $[WOCl_3\{MeS\{CH_2)_nSMe]$, both of which were identified crystallographically. Curiously, they are geometric isomers: $[WOCl_3\{MeS(CH_2)_3SMe\}]$ has the dithioether *trans* Cl/Cl whereas in $[WOCl_3\{MeS(CH_2)_2SMe\}]$ it is *trans* O/Cl.

Remarkably, low pressure chemical vapour deposition (CVD) experiments using the dinuclear W(VI) species, $[(WSCl_4)_2\{^iPrS(CH_2)_2S^iPr\}]$, as a single source precursor produced thin films of 4H-WS_2, identified by grazing incidence X-ray diffraction, scanning electron microscopy, X-ray photoelectron spectroscopy and Raman spectroscopy; the tungsten thiochloride complex is the first single source low pressure CVD precursor for WS_2. In contrast, the mononuclear W(V) complex, $[WSCl_3\{^iPrS(CH_2)_2S^iPr\}]$, does not deposit WS_2 under similar conditions.

Introduction

The synthesis and some limited coordination chemistry of early 4d and 5d thiohalides, including $NbSX_3$, $TaSX_3$, WSX_4, $MoSCl_3$ and WSX_3 (X = Cl or Br), was first explored in the period 1965-1985, much of it by Fowles, Rice and Drew,[1-3] who showed the thiohalides were moderate Lewis acids towards neutral N- or O-donor ligands. Their chemistry was generally similar to that of the corresponding oxide halides, although the thiohalide species seemed more limited and less stable. Complexes of WOF_4 and WSF_4 have been explored more recently,[4,5] but MSF_3 (M = Nb or Ta) are unknown. We recently reported a series of thioether complexes of $NbSCl_3$, of type $[NbSCl_3(SR_2)]$ (R = Me, ^nBu), obtained from reaction of $NbCl_5$, SR_2 and $S(SiMe_3)_2$ in CH_2Cl_2. [6] The structure of the $[Nb_2S_2Cl_6(SMe_2)_2]$ revealed a Cl-bridged dimer with the SMe_2 ligands disposed *syn*. The six-coordinate dithioether analogues, $[NbSCl_3(L–L)]$ (L–L = $MeS(CH_2)_2SMe$, $MeS(CH_2)_3SMe$, $^iPrS(CH_2)_2S^iPr$ and $^nBuS(CH_2)_3S^nBu$), were obtained from reaction of L–L with preformed $[NbSCl_3(MeCN)_2]$. We also showed that selected examples can function as single source precursors for low pressure chemical vapour deposition (LPCVD) of thin films of 3R-NbS_2.[6] These were the first examples of single source LPCVD reagents using complexes based upon thiohalide M=S units. However, attempts to use analogous thioether complexes of $TaSCl_3$ did not produce TaS_2 deposition.[7]

We have reported elsewhere the synthesis, spectroscopic properties and X-ray crystal structures of a range of six-coordinate complexes of $WSCl_4$ (and analogues with $WOCl_4$) with some hard donor phosphine oxides and pyridyl ligands,[8] and highly unusual, seven-coordinate (pentagonal bipyramidal) W(VI) complexes with phosphine and arsine coordination, $[WECl_4\{o\text{-}C_6H_4(QMe_2)_2\}]$ (E = O, S, Q = P, As).[9]

Layered early transition metal dichalcogenides, ME_2 (M = Nb, Ta, V, W, *etc*.; E = S, Se or Te) are more stable inorganic analogues of graphene, and their properties and band gaps can be tuned by varying the metal and the chalcogen.[10] Applications of these materials include in optoelectronics, spintronics, sensors, electrocatalysis and magnetic materials. [10-12] Chemical vapour deposition (CVD) is a low cost and versatile method to deposit such films, using either dual or single source precursors, with single source precursors offering the prospect of better control of film stoichiometry and efficient use of reagents.[13,14] To our knowledge there are no single source precursors for low pressure CVD of WS_2. Aerosol-assisted CVD (AACVD) of WS_2 from the dithiocarbamate complex, $[WS(S_2)(S_2CNEt_2)_2]$, and of $Mo_{1-x}W_xS_2$ from a mixture of $[WS_3\{S_2CN(Et_2)_2\}_2]$ and $[Mo\{S_2CN(Et_2)_2\}_4]$ have been reported very recently.[15] Routes to WS_2 films typically include sulfurisation of WO_3 at elevated temperature, or using dual source precursors, such as WF_6 and H_2S, or WCl_6, $WOCl_4$ or $W(CO)_6$ with thiols.[16]

Here we report the synthesis, spectroscopic and structural studies of a series of thioether complexes of $WSCl_4$ and $WSCl_3$ alongside a comparative study of their $WOCl_4$ analogues. We also report on our evaluation of $[(WSCl_4)_2\{^iPrS(CH_2)_2S^iPr\}]$ and $[WSCl_3\{^iPrS(CH_2)_2S^iPr\}]$ as potential single source precursors for the growth of WS_2 thin films by low pressure CVD.

Previous work has shown that the reaction of $WSCl_4$ with 0.5 equivalents of $MeS(CH_2)_2SMe$ forms $[\{WSCl_4)_2\{MeS(CH_2)_2SMe\}]$,[17] the crystal structure of which showed the dithioether bridge linking two six-coordinate tungsten centres.[18] Use of an excess of the dithioether or long reaction times caused reduction to tungsten(V) with a chelating dithioether ligand, as in $[WSCl_3\{MeS(CH_2)_2SMe\}]$.[19]

Experimental

Syntheses were performed using standard Schlenk and glove-box techniques under a dry N_2 atmosphere. WCl_6 (Acros organics), $O(SiMe_3)_2$ and $S(SiMe_3)_2$ (Sigma-Aldrich) were used as received. Solvents were dried by distillation from CaH_2 (CH_2Cl_2, MeCN) or Na/benzophenone ketyl (toluene, n-hexane). The monodentate ligands (SMe_2, SPh_2, $SeMe_2$) were obtained from Sigma-Aldrich or Strem and dried over molecular sieve. The dithioethers,[20] $WOCl_4$ and $WSCl_4$ were made as described elsewhere.[8,21]

Infrared spectra were recorded on a Perkin-Elmer Spectrum 100 spectrometer in the range 4000–200 cm^{-1}, with samples prepared as Nujol mulls between CsI plates. ^1H NMR spectra were recorded using a Bruker AV 400 spectrometer and referenced to the residual protio-resonance of the solvent. $^{77}Se\{^1H\}$ NMR spectra were obtained from CD_2Cl_2 solutions using a Bruker AV 400 spectrometer and referenced to neat $SeMe_2$. Spectra were recorded at 295 K unless indicated otherwise. UV/ visible spectra were recorded as powdered solids, using the diffuse reflectance attachment of a PerkinElmer 750S spectrometer. Microanalyses on new compounds were undertaken by London Metropolitan University.

$[(WSCl_4)_2\{MeS(CH_2)_2SMe\}]$: A solution of 2,5-dithiahexane (0.026 g, 0.21 mmol) in dichloromethane (5 mL) was slowly added to a suspension of $WSCl_4$ (0.150 g., 0.42 mmol) in dichloromethane (5 mL). The dark red solution was then stirred for 1 h, concentrated *in vacuo* to ~ 3 mL, filtered, and the red/brown solid dried *in vacuo.* Yield: 0.050 g, 28%. Required for $C_4H_{10}Cl_8S_4W_2$ (837.7): C: 5.74, H: 1.25. Found: C: 5.83, H: 1.19%. IR spectrum (Nujol / cm^{-1}): 534s W=S, 376m, 335s W-Cl. ^1H NMR (CD_2Cl_2): δ = 2.98 (s, [2H], CH_2), 2.32 (s, [3H], CH_3). UV/Vis spectrum (diffuse reflectance) / cm^{-1}: 35,350, 32,250 sh, 20,200.

$[(WSCl_4)_2\{MeS(CH_2)_3SMe\}]$: Prepared similarly using 2,6-dithiaheptane (0.029 g, 0.21 mmol) and $WSCl_4$ (0.150 g, 0.42 mmol). Red/brown solid. Yield: 0.096 g, 54%. Required for $C_5H_{12}Cl_8S_4W_2$ (851.7): C: 7.05, H: 1.42. Found: C: 7.24, H: 1.53%. IR spectrum (Nujol / cm^{-1}): 529s W=S, 360m, 332s W-Cl.

^1H NMR (CD_2Cl_2): δ = 2.72 (s br, [4H], SCH_2), 2.20 (s br, [6H], CH_3), 2.03 (s br, [2H], CH_2). UV/Vis spectrum (diffuse reflectance) / cm^{-1}: 34,750, 32,200, 20,000.

[$(WSCl_4)_2\{^iPrS(CH_2)_2S^iPr\}$]: Prepared similarly using 1,2-bis(isopropylthio)ethane (0.037 g, 0.21 mmol) and $WSCl_4$ (0.150 g, 0.42 mmol). Red/brown solid. Yield: 0.101 g, 54%. Required for $C_8H_{18}Cl_8S_4W_2$ (893.8): C: 10.75, H: 2.03. Found: C: 10.90, H: 1.95. IR spectrum (Nujol / cm^{-1}): 543s W=S, 370m 341s W-Cl. ^1H NMR (CD_2Cl_2): δ = 3.15 (sep, [2H]. CH, $^3J_{HH}$, 8Hz), 2.86 (s, [2H], CH_2), 1.32 (d, [6H], $^3J_{HH}$, 8Hz, CH_3). UV/Vis spectrum (diffuse reflectance) / cm^{-1}: 36,500, 32,250, 20,800.

[$(WSCl_4)_2\{PhS(CH_2)_2SPh\}$]: Made similarly using 1,2-bis(phenylthio)ethane (0.052 g, 0.21 mmol) and $WSCl_4$ (0.150 g, 0.42 mmol) in toluene. Dark red solid. Yield: 0.090 g, 45%. Required for $C_{14}H_{14}Cl_8S_4W_2$ (961.82): C: 17.48, H: 1.47. Found: C: 17.52, H: 1.60%. IR spectrum (Nujol / cm^{-1}): 539s W=S, 355m, 337s W-Cl. ^1H NMR (CD_2Cl_2): δ = 7.33 (br, [10H], Ph), 3.20 (s br, [4H], CH_2).

[$WSCl_4(SMe_2)$]·CH_2Cl_2: Made similarly using dimethylsulfide (0.026 g, 0.42 mmol) and $WSCl_4$ (0.150 g, 0.42 mmol). Brown/red solid. Yield: 0.101 g, 48%. Required for $C_2H_6Cl_4S_2W\cdot CH_2Cl_2$ (504.78): C: 7.14, H: 1.60. Found: C: 7.26, H: 1.73%. IR spectrum (Nujol / cm^{-1}): 538s W=S, 347s W-Cl. ^1H NMR (CD_2Cl_2): δ = 2.32 (s, br, SMe_2), 5.32 (s, CH_2Cl_2).

[$WSCl_4(SeMe_2)$]: Made similarly using dimethylselenide (0.046 g, 0.42 mmol) and $WSCl_4$ (0.150 g, 0.42 mmol). Brown solid. Yield: 0.134 g, 68%. Required for $C_2H_6Cl_4SSeW$ (466.75): C: 5.15, H: 1.30. Found: C: 5.22, H: 1.36%. IR spectrum (Nujol / cm^{-1}): 525s W=S, 331m W-Cl. ^1H NMR (CD_2Cl_2): δ = 2.23 (s). $^{77}Se\{^1H\}$ NMR (CD_2Cl_2, 295 K): no resonance; (183 K): δ = +81.3.

[$(WOCl_4)_2\{PhS(CH_2)_2SPh\}$]: Made similarly using 1,2-bis(phenylthio)ethane (0.054 g, 0.22 mmol) and $WOCl_4$ (0.150 g, 0.44 mmol). Dark pink solid. Yield: 0.070 g, 34%. Required for $C_{14}H_{14}Cl_8O_2S_2W_2$ (929.69): C: 18.09, H: 1.52. Found: C: 18.18, H: 1.60%. IR spectrum (Nujol / cm^{-1}): 992s, 982s W=O, 356s W-Cl. ^1H NMR (CD_2Cl_2): δ = 7.39 (m, [10H], Ph), 3.43 (s, [4H], CH_2).

[$(WOCl_4)_2\{^iPrS(CH_2)_2S^iPr\}$]: Made similarly using 1,2-bis(isopropylthio)ethane (0.039 g, 0.22 mmol) and $WOCl_4$ (0.150 g, 0.44 mmol). Greenish-brown solid. Yield: 0.089 g, 47%. Required for $C_8H_{18}Cl_8O_2S_2W_2$ (861.6): C: 11.15, H: 2.11 Found: C: 11.24, H: 2.14%. IR spectrum (Nujol / cm^{-1}): 998s W=O, 352s W-Cl. ^1H NMR (CD_2Cl_2): δ = 3.20 (sep, [2H], $^3J_{HH}$ 8 Hz, CH), 2.90 (s, [2H], CH_2), 1.34 (d, [6H], $^3J_{HH}$ 8 Hz, CH_3).

[$WOCl_4(SMe_2)$]: Made similarly using dimethylsulfide (0.027 g, 0.44 mmol) and $WOCl_4$ (0.150 g, 0.44 mmol). Brown-yellow solid. Yield: 0.096 g, 54%. Required for $C_2H_6Cl_4OSW$ (403.8): C: 5.95, H: 1.50.

Found: C: 5.86, H: 1.39%. IR spectrum (Nujol / cm^{-1}): 993s, W=O, 352s W-Cl. ^{1}H NMR (CD_2Cl_2): δ = 2.54 (s, br).

[$WSCl_3${MeS(CH_2)$_2$SMe}]: Made similarly using 2,5-dithiahexane (0.051 g, 0.42 mmol) and $WSCl_4$ (0.150 g, 0.42 mmol). Red/brown solid. Yield: 0.070 g, 37%. Required for $C_4H_{10}Cl_3S_3W$ (444.5): C: 10.81, H: 2.27. Found: C: 11.07, H: 2.26%. IR spectrum (Nujol / cm^{-1}): 528m W=S, 329s, br W-Cl.

[$WSCl_3${^{i}PrS(CH_2)$_2$S^{i}Pr}]: Made similarly using 1,2-bis(isopropylthio)ethane (0.112 g, 0.63 mmol) and $WSCl_4$ (0.150 g, 0.42 mmol). Red/brown solid. Yield: 0.170 g, 81%. Required for $C_8H_{18}Cl_3S_3W$ (500.62): C: 19.19, H: 3.62. Found: C: 19.50, H: 3.77%. IR spectrum (Nujol / cm-1): 527s W=S, 340m, 323s W-Cl.

X-ray experimental

Data collections used a Rigaku AFC12 goniometer equipped with an enhanced sensitivity (HG) Saturn724+ detector mounted at the window of an FR-E+ SuperBright molybdenum (λ = 0.71073) rotating anode generator with VHF Varimax optics (70 micron focus) with the crystal held at 100 K (N_2 cryostream). Crystallographic parameters are presented in Table 1. Structure solution and refinement were performed using SHELX(T)-2018/2, SHELX-2018/3 through Olex2[22] and were mostly straightforward, although some of the structures showed significant residual electron peaks near to the tungsten, which are attributed to absorption correction problems. The [$WSCl_3${MeS(CH_2)$_2$SMe}] showed Cl/S disorder, which was modelled by a split atom occupancy approach, occupancies modelled as free variable and then fixed at 0.25 and 0.75. Atoms in the same site were constrained with EADP.

LPCVD of WS_2 films using [($WSCl_4$)$_2${^{i}PrS(CH_2)$_2$S^{i}Pr}]

The precursor (20-30 mg) was loaded into the precursor bulb at the closed end of a silica tube in a N_2 purged glove box, silica substrates (*ca.* 1 x 8 x 20 mm^3) were then positioned end-to-end lengthways along the tube outwards from the precursor. The tube was then set in a furnace so that the substrates were in the heated zone and the precursor protruded *ca.* 1 cm outside the furnace. The tube was evacuated to 0.1 mm Hg and the furnace heated to 700 °C and left for 10 mins. to allow the temperature to stabilise. The tube was gradually moved towards the hot zone until evaporation of the precursor began and the position was maintained until no further evaporation occurred, leaving some black solid in the precursor bulb. After *ca.* 20 min. the tube was cooled to room temperature and the substrates were unloaded in the glove box where they were stored for characterisation. Brown/bronze films were observed on the substrates in the hot zone between 590-625 °C (determined by temperature profiling), i.e. 1.5-3.5 cm away from the precursor.

Film Characterisation: X-ray diffraction (XRD) patterns were collected in grazing incidence mode (θ1 = 1°) using a Rigaku SmartLab diffractometer (Cu-Kα, λ = 1.5418 Å) with parallel X-ray beam and a DTex Ultra 250 detector operated in 1D mode. Phase matching and lattice parameter calculations (WS_2) used the PDXL2 software package[27] and diffraction patterns from ICSD.[23] High resolution scanning electron microscopy (SEM) measurements were carried out with a field emission SEM (Jeol JSM 7500F) at an accelerating voltage of 2 kV. X-ray photoelectron spectroscopy (XPS) data were obtained using a ThermoScientific Theta Probe system with Al–Kα radiation (photon energy= 1486.6 eV). All peak are calibrated against the adventitious C1s peak at 284.6eV. Raman spectra of the deposited films were measured at room temperature on a Renishaw InVia Micro Raman Spectrometer using 532 nm excitation. The incident laser power was adjusted to 0.1 mW for all samples.

Results and Discussion

$WSCl_4$ complexes: The $WSCl_4$ was made as reported[8,21] from reaction of WCl_6 and $S(SiMe_3)_2$ in anhydrous CH_2Cl_2 and purified by sublimation *in vacuo.* Subsequent reaction of $WSCl_4$ with the dithioethers, $RS(CH_2)_2SR$ (R = Me, Ph, ^iPr) and $MeS(CH_2)_3SMe$, in anhydrous CH_2Cl_2 in a 2:1 molar ratio and with short reaction times gave the dinuclear W(VI) products $[(WSCl_4)_2\{RS(CH_2)_nR\}]$ as red-brown solids in moderate yields (Scheme 1).

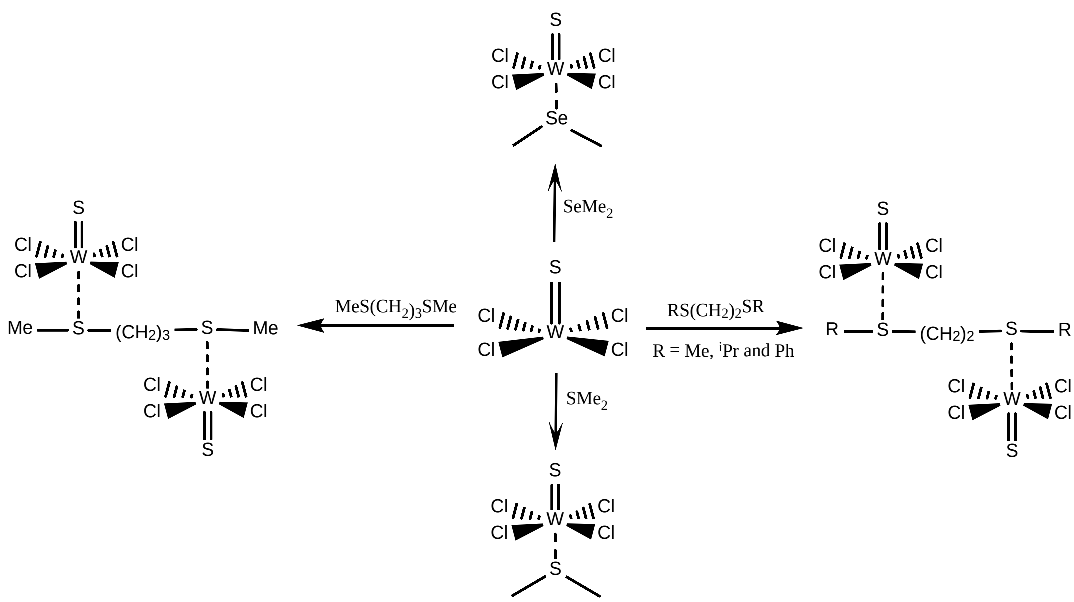

Scheme 1. Synthesis of the complexes of $WSCl_4$.

The complexes are easily hydrolysed, but can be prepared and handled using dry solvents via glove box and Schlenk line techniques and the solids are not degraded even over several months if stored in a dry N_2-purged glove box. If the reaction of $WSCl_4$ with $RS(CH_2)_2SR$ (R = Me, ^{i}Pr) is carried out with a 1:1 molar ratio, or if longer reaction times are used, reduction to W(V) occurs to give the complexes, [$WSCl_3${$RS(CH_2)_2SR$}] (see below). Crystals of all four W(VI) dithioether complexes were obtained by slow evaporation from CH_2Cl_2 solutions in the glove box and single crystal X-ray analysis confirmed the formation of the ligand bridged dimers, as formulated above (Figs. 1a-c, S1). The structure of [{$WSCl_4$}$_2${$MeS(CH_2)_2SMe$}] has been reported previously[17]; the present structure, which is of higher precision, is included in the ESI (Fig. S1). All of the structures show the hexavalent tungsten in a distorted octahedral environment, with the W=S lying *trans* to the neutral sulfur donor atom and with the four equatorial chlorines bent away from the W=S unit; the corresponding W=S (~2.09 Å), W-S (~ 2.84 Å) and W-Cl (~2.31 Å) bond lengths are very similar across the series.

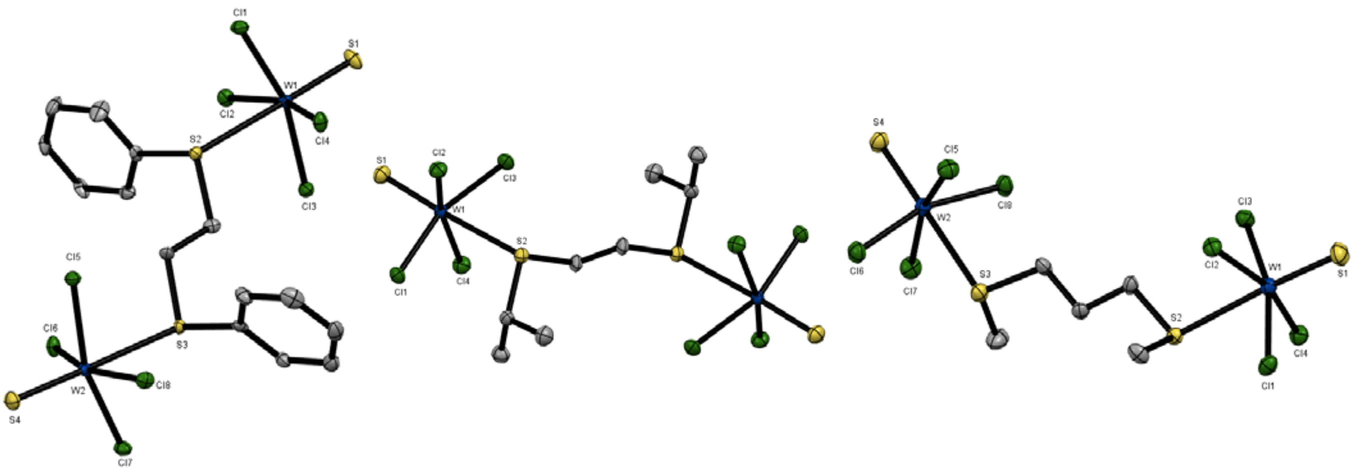

(a) **(b)** **(c)**

Figure 1. The structures with atom numbering scheme (H atoms are omitted for clarity and ellipsoids are shown at the 50% probability level) of **(a)** [($WSCl_4$)$_2${$PhS(CH_2)_2SPh$}]: selected bond lengths (Å) and angles (°) are W2–Cl6 = 2.3180(16), W2–Cl7 = 2.3157(18), W2–Cl8 = 2.2891(16), W2–Cl5 = 2.3143(18), W1–Cl2 = 2.2849(16), W1–Cl4 = 2.3213(16), W1–Cl1 = 2.3148(18), W1–Cl3 = 2.3041(18), W1–S2 = 2.8600(16), W1–S1 = 2.1003(17), W2–S3 = 2.8635(16), W2–S4 = 2.1039(17), S1–W1–Cl(1-4) = 99.51(7) –100.37(6), S4–W2–Cl(5-8) = 97.30(7) – 101.17(7); **(b)** [($WSCl_4$)$_2${^{i}PrS$(CH_2)_2$S^{i}Pr}]: selected bond lengths (Å) and angles (°) are W1–Cl2 = 2.3231(17), W1–Cl1 2.3100(17), W1–Cl4 = 2.3155(17), W1–Cl3 = 2.3096(17), W1–S1 = 2.0967(19), W1–S2 = 2.8633(18), S1–W1–Cl(1-4) = 97.87(7) –100.13(7), S2–W1–Cl(1-4) = 78.29(6) – 85.01(6); **(c)** [($WSCl_4$)$_2${$MeS(CH_2)_3SMe$}]: selected bond lengths (Å) and angles (°) are W2–Cl6 = 2.325(2), W2–Cl7 = 2.291(2)), W2–Cl8 = 2.312(2), W2–Cl5 = 2.323(2), W1–Cl2 = 2.307(2), W1–Cl4 = 2.320(2), W1–Cl1 = 2.295(2), W1–Cl3 = 2.329(2), W1–S2 = 2.816(2), W1–S1 = 2.102(2), W2–S3 = 2.808(2), W2–S4 = 2.109(2), S1–W1–Cl(1-4) = 98.54(9) –100.30(9), S4–W2–Cl(5-8) = 98.91(9) – 99.62(8).

The IR spectra of the [($WSCl_4$)$_2${dithioether}] complexes each show a strong band in the range 530-545 cm^{-1} assigned as ν(W=S). A strong band ~ 335 cm^{-1} and a medium intensity feature ~ 370 cm^{-1} are assigned as the e and a_1 ν(W–Cl) modes, respectively, consistent with the solid state structures.

The diffuse reflectance UV/visible spectra show strong overlapping absorptions, which, from comparison with the spectrum of $WSCl_4$ itself,[24] may be assigned as charge transfer Cl→W (~36,000, ~ 32,500 cm^{-1}) and S→W (~ 20,000 cm^{-1}) transitions; the lack of any absorptions at lower energy found in W(V) complexes[25] confirms the oxidation state as W(VI), as formulated. The ^1H NMR spectra, obtained from rigorously anhydrous CD_2Cl_2 solutions, show the presence of symmetrically coordinated dithioethers, with the expected high frequency coordination shifts.

The red-brown mononuclear [$WSCl_4(SMe_2)$] was also isolated from the reaction of $WSCl_4$ and SMe_2 (1 : 1 molar ratio) in CH_2Cl_2 and shows very similar spectroscopic features to the dinuclear dithioether complexes, but no reaction was apparent between the less basic SPh_2 and tungsten thiochloride.

The formation of complexes of $WSCl_4$ with the heavier selenoether ligands was also briefly examined. Brown [$WSCl_4(SeMe_2)$], obtained from reacting $WSCl_4$ and $SeMe_2$ in CH_2Cl_2 solution, shows ν(W=S) at 525 cm^{-1} and ν(W–Cl) at 331 cm^{-1} by IR spectroscopy, while its ^1H NMR spectrum (CD_2Cl_2) is a singlet at $\delta = 2.23$, a significant high frequency shift from $SeMe_2$ itself ($\delta = 1.93$), indicative of complexation. No $^{77}Se\{^1H\}$ NMR resonance was seen at room temperature, presumably due to fast exchange on the NMR timescale, but at 183 K the solution showed a single resonance at $\delta = +81.3$, a large coordination shift from 'free' $SeMe_2$ ($\delta = 0$), also consistent with coordination to W(VI). Several attempts to isolate a $WSCl_4$ complex with $MeSe(CH_2)_2SeMe$ using similar reaction conditions were unsuccessful.

$WSCl_3$ complexes: Two examples of the (reduced) W(V) complexes, [$WSCl_3\{RS(CH_2)_2SR\}$] (R = Me, ^{i}Pr) were obtained using a $WSCl_4$: ligand ratio of 1: ≥ 1 and/or heating the reaction mixture. The products are red-brown paramagnetic solids. In the IR spectra both the ν(W=S) and ν(W-Cl) are at slightly lower frequency than the values in the in the W(VI) complexes discussed above. The ν(W-Cl) will be affected by the different symmetry of the two complex types, but in both complexes the W=S is *trans* to a neutral thioether donor.

The crystal structure of [$WSCl_3\{MeS(CH_2)_2SMe\}$] was reported in early work,[19] but was redetermined here to obtain higher precision data to allow comparison with the W(VI) analogues described above. The structure (Fig. 4) confirms a distorted octahedral geometry with the chelating dithioether lying *trans* to S/Cl. It also showed S/Cl disorder in the equatorial plane that was satisfactorily modelled using split atoms sites, which were refined to occupancies of 0.25 : 0.75; only the major component is shown in Fig. 2. Because of the disorder present, comparison of bond lengths must be made with care, but the d(W=S) appears to be little different to the values in the W(VI) analogues, whilst d(W-

Cl) is slightly longer in the W(V) complex. The d(W-S) in the latter show a marked effect of the *trans* donor, W1–S3 (*trans* to W=S) = 2.501(1) Å, W1–S2 (*trans* to W-Cl) = 2.764(1) Å.

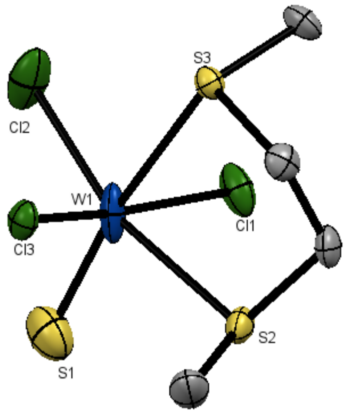

Figure 2 The structure of [$WSCl_3\{MeS(CH_2)_2SMe\}$] showing the atom numbering scheme and ellipsoids are shown at the 50% probability level. Note that there is S/Cl disorder in plane, which was modelled as split atom sites 0.25 : 0.75; only the major form is shown. Selected bond lengths (Å) and angles (°) are: W1–S3 = 2.5010(13), W1–S2 = 2.7644(13), W1–Cl2 = 2.3594(12), W1–Cl3 = 2.3494(13), W1–Cl1 = 2.315(2), W1–S1 = 2.054(5), Cl2–W1–S2 = 76.92(4), Cl2–W1–S3 = 90.01(4), Cl3–W–1S2 = 84.76(4), Cl3—W1–S3 = 82.49(5), Cl1–W1–S2 = 83.36(6), Cl1–W1–Cl2 = 90.69(6), Cl1–W1–Cl3 = 91.34(7), S1–W1–S3 = 93.48(18), S1–W1–Cl2 = 100.16(15), S1–W–1Cl3 = 97.49(16), S1–W1–Cl1 = 103.82(18), S3–W1–S2 = 79.55(4).

$WOCl_4$ and $WOCl_3$ complexes: The reaction of $WOCl_4$ with a similar set of thioether ligands was also explored to provide some comparisons with the $WSCl_4$ complexes described above (Scheme 2).

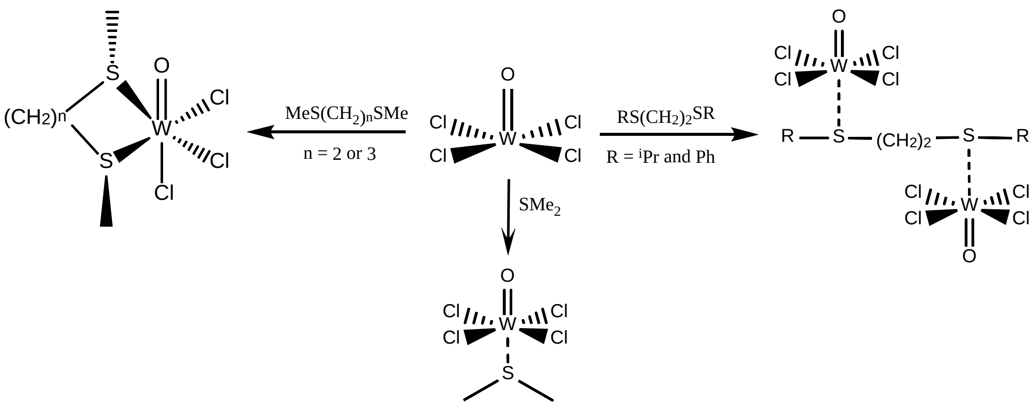

Scheme 2. Synthesis of $WOCl_4$ complexes

Direct reaction of $WOCl_4$ with $RS(CH_2)_2SR$ (R = ^{i}Pr, Ph) readily afforded the dinuclear [$(WOCl_4)_2\{\mu\text{-}RS(CH_2)_2SR\}$]. However, while the $MeS(CH_2)_nSMe$ (n = 2, 3) appeared to form analogous complexes, these were unstable and could not be obtained as analytically pure samples, the products isolated always appearing to contain a mixture of W(VI) and W(V) complexes. A greenish-brown W(VI) monomer, [$WOCl_4(SMe_2)$], was isolated from CH_2Cl_2 solution using a 1:1 molar ratio of reagents. The IR spectrum of green [$(WOCl_4)_2\{\mu\text{-}^iPrS(CH_2)_2S^iPr\}$] exhibits ν(W=O) at 998 cm^{-1} and ν(W-Cl) at 325 cm^{-}

[1], similar values to those found in the phosphine oxide or pyridine complexes.[8] The spectrum of $[(WOCl_4)_2\{\mu\text{-PhS}(CH_2)_2SPh\}]$ is similar, except that two ν(W=O) bands at 992 and 982 cm^{-1} were observed. Neither of the bands correspond to a thioether ligand mode and the small splitting is ascribed to a solid-state effect.

The tungsten(VI) oxide tetrachloride complexes of dithiahexane and dithiaheptane could not be isolated (above), but the mixtures in CH_2Cl_2 produced a few crystals of the reduced W(V) complexes, $[WOCl_3\{MeS(CH_2)_nSMe\}]$ (n = 2, 3) (Figs. 3a and b).

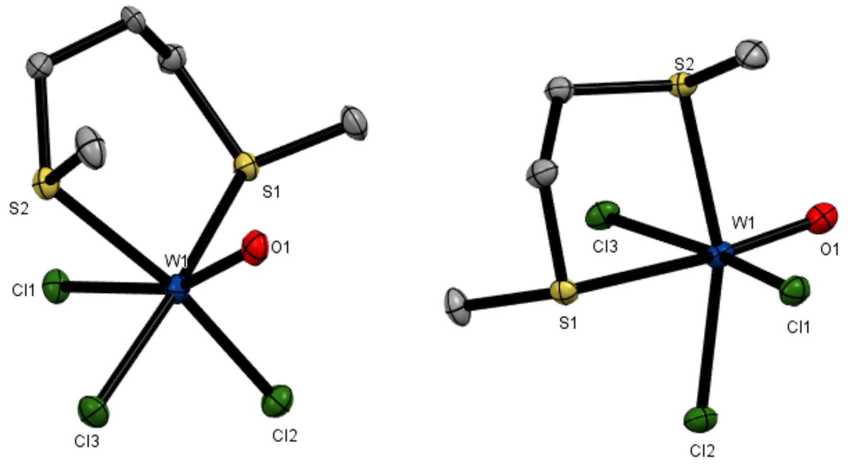

(a) (b)

Figure 3 The structures, showing the atom numbering scheme (H atoms are omitted for clarity and ellipsoids are shown at the 50% probability level), of **(a)** $[WOCl_3\{MeS(CH_2)_3SMe\}]$: selected bond lengths (Å) and angles (°) are W1–Cl1 = 2.3602(17), W1–Cl2 = 2.3316(16), W1–Cl3 = 2.4639(16), W1–S2 = 2.5213(17), W1–S1 = 2.5185(17), W1–O1 = 1.720(5), O1–W1–Cl1 = 100.32(17), O1–W1–Cl2 = 102.31(16), O1–W1–S1 = 89.29(16), O1–W1–S2 = 89.37(16), Cl1–W1–Cl3 = 93.29(6), Cl1–W1–S2= 85.14(6), Cl2–W1–Cl1 = 92.19(6), Cl2–W1–S1 = 83.38(6), Cl2–W1–Cl3 = 91.63(6), S1–W1–S2 = 97.42(6), Cl3–W1–S1 = 78.06(5), Cl3—W1–S2 = 77.19(5); **(b)** $[WOCl_3\{MeS(CH_2)_2SMe\}]$: selected bond lengths (Å) and angles (°) are: W1–Cl1 = 2.359(4), W1–Cl2 = 2.337(3), W1–S1 = 2.758(3), W1–S2 = 2.520(3), W1–Cl3 = 2.358(4), W1–O1 = 1.729(12), Cl1–W1–S1 = 77.13(14), Cl1–W1–S2 = 90.72(13), Cl2–W1–Cl1 = 91.68(13), Cl2–W1–S1 = 82.17(13), Cl2–W1–Cl3 = 89.99(13), S2–W1–S1 = 79.81(12), Cl3–W1–S1 = 85.91(13), Cl3–W1–S2 = 82.20(13), O1–W1–Cl1 = 98.4(4), O1–W1–Cl2 = 105.1(4), O1–W1–S2 = 93.4(4), O1–W1–Cl3 = 98.0(4).

Both structures are based upon *pseudo*-octahedrally coordinated tungsten with the dithioether chelating, but are different geometric isomers; $[WOCl_3\{MeS(CH_2)_2SMe\}]$ has the neutral dithioether ligand *trans* O/Cl, whilst in $[WOCl_3\{MeS(CH_2)_3SMe\}]$ the dithioether is *trans* Cl/Cl. The isomers found in many MEX_3L_2 and MEX_3(L-L) (E = O, S; X = halide) have the neutral ligand(s) *trans* E/X and frequently show E/X disorder in plane.[1,3,6,7,26] There is no evidence for disorder in the crystal structure of $[WOCl_3\{MeS(CH_2)_2SMe\}]$.

Tungsten disulfide films grown by low pressure CVD:

The successful isolation of the series of the tungsten(VI) and (V) thiochloride complexes bearing thioether co-ligands described above raised the prospect that it may be possible to use some of these as single source CVD precursors for the growth of technologically relevant tungsten disulfide thin films. In order to test this hypothesis, the complexes selected were those containing ^{i}Pr substituents in the thioether ligands, in order to provide a low energy decomposition pathway via β-hydride elimination.[6,27] We found that low pressure CVD experiments in the temperature range 600-700 °C (0.1 mmHg) using the dinuclear W(VI) complex, $[(WSCl_4)_2\{^{i}PrS(CH_2)_2S^{i}Pr\}]$, indeed led to deposition of bronze-coloured, reflective thin films across the substrate tiles positioned 1.5-3.5 cm from the precursor (i.e. in the temperature range 590-625 °C), the identification and characterisation of which is described below; unsurprisingly, some intractable dark residue also remained in the precursor bulb at the end of the experiments.

Notably, in contrast, the $[WSCl_3\{^{i}PrS(CH_2)_2S^{i}Pr\}]$ failed to produce any visible deposit on the tiles under comparable conditions, suggesting that this W(V) species is not a suitable CVD precursor under these conditions.

Characterisation of the bronze films obtained from the $[(WSCl_4)_2\{^{i}PrS(CH_2)_2S^{i}Pr\}]$ precursor was attempted using a grazing incidence X-ray diffraction (XRD), scanning electron microscopy (SEM), X-ray photoelectron spectroscopy (XPS) and Raman spectroscopy.

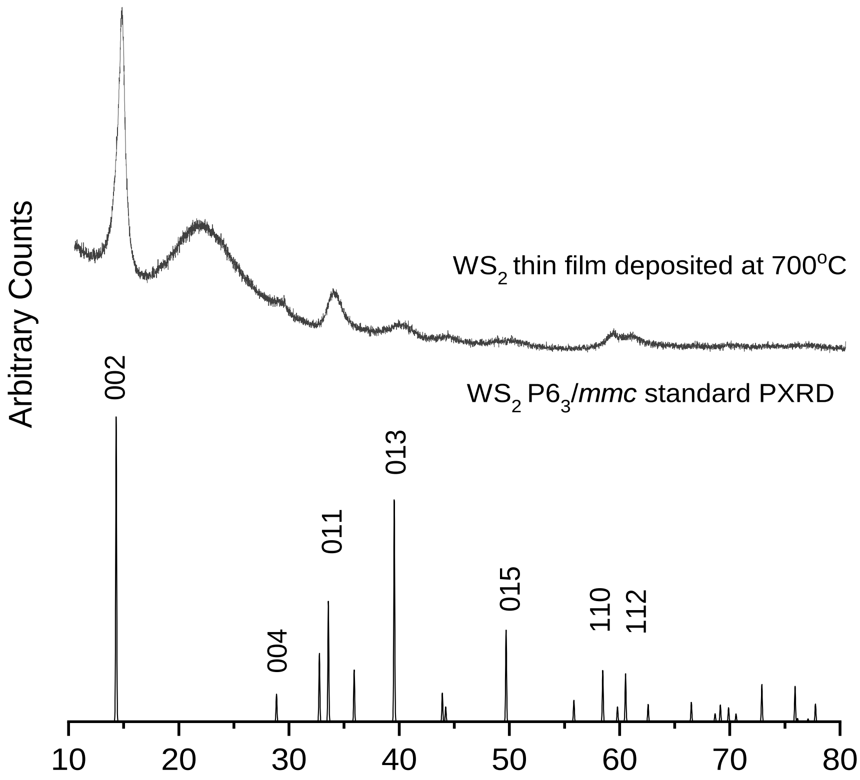

d

Figure 4 Grazing incidence XRD pattern (top) from a WS_2 thin film deposited by low pressure CVD using [$(WSCl_4)_2${^{i}PrS$(CH_2)_2$S^{i}Pr}] at 700°C / 0.1 mmHg. The broad feature at 2θ = 20-25 ° is from the SiO_2 substrate. XRD pattern for bulk WS_2 (bottom).[28]

Grazing incidence XRD analysis of the films obtained from the dinuclear [$(WSCl_4)_2${^{i}PrS$(CH_2)_2$S^{i}Pr}] (deposited at 700°C / 0.1 mmHg) (Fig. 4) are consistent with polycrystalline 4H WS_2 in space group P6$_3$/*mmc*. Lattice parameters were refined as: a = 3.1523(11), c = 12.381(4) (R_{wp} = 7.67%, literature: a = 3.1532(4); c = 12.323(5) Å).[28] The grazing incidence diffraction patterns are dominated by the 002 reflection, suggesting a preferred orientation in the <00*l*> direction. This is not unusual, as these layered materials typically grow initially with the *c* axis normal to the substrate and suggests that the majority of the platelet crystals have grown in that orientation, with platelets flat to the substrate. The films were too thin to allow an in plane XRD measurement even over an extended period. The average crystallite size in the WS_2 film was calculated from the grazing incidence XRD data in Fig. 4 using the Williamson-Hall method, giving an estimated size of 9.1(3) nm. Scanning electron microscopy showed uniform and continuous coverage across the substrate by small hexagonal platelet crystallites (Fig. 5).

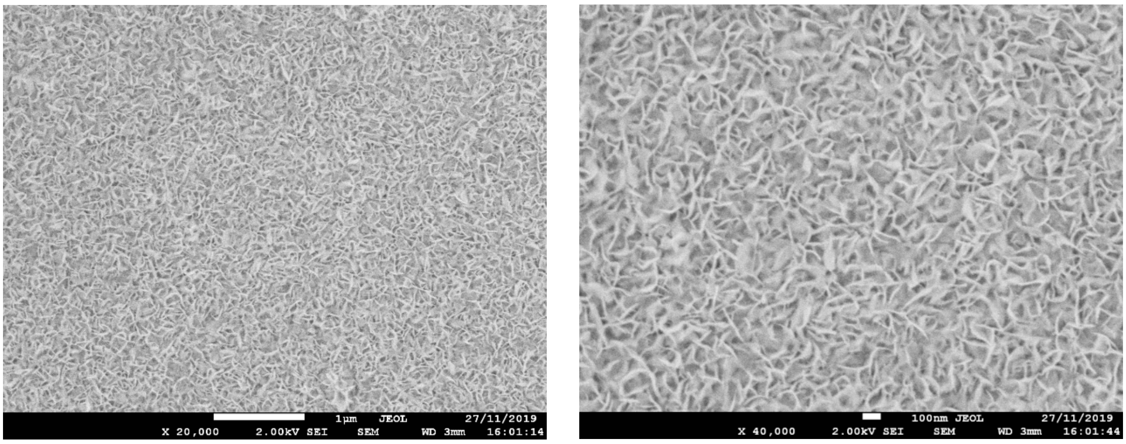

Figure 5. SEM images of a continuous WS_2 thin film produced via low pressure CVD using $[(WSCl_4)_2\{^iPrS(CH_2)_2S^iPr\}]$

Accurate determination of the composition by energy dispersive X-ray (EDX) analysis was not possible due to overlap of the peaks due to tungsten with those from silicon in the substrate, as well as the beam penetration into the substrate, however, X-ray photoelectron spectroscopy (XPS) analysis on the as-deposited films are shown in Fig. 6. The W peaks at 32.6, 34.7, 38.2 eV can be assigned to W 4f7/2, W 4f5/2, W 5p3/2, from which it can be concluded that the films are not oxidized.[29] The S peaks at 162.2 and 163.4eV are attributed to S 2p1/2 and S 2p3/2 and are characteristic of S^{2-} in WS_2. The W:S ratio (1 : 2.2) was estimated by integrating the W4f and S2p peaks.

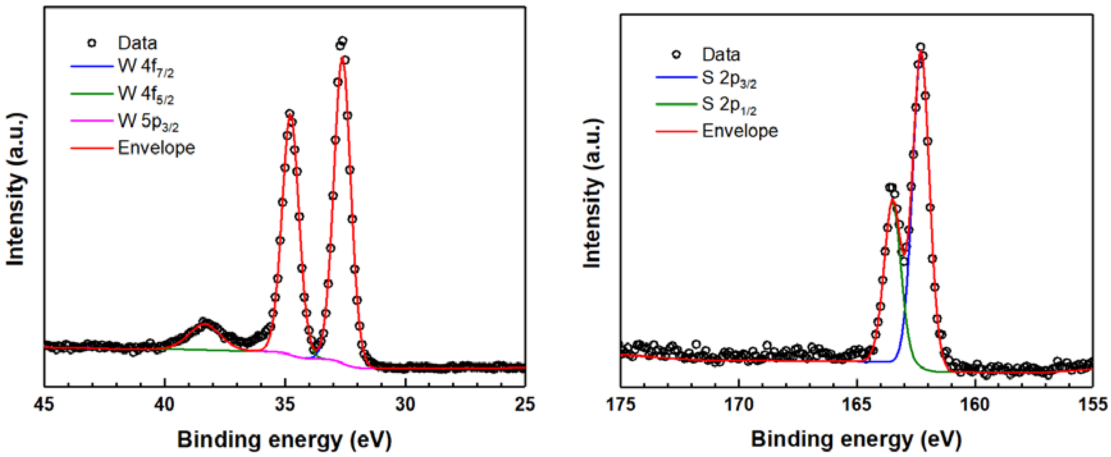

Figure 6 Representative XPS data for an as-deposited WS_2 film obtained using $[(WSCl_4)_2\{^iPrS(CH_2)_2S^iPr\}]$ showing the peaks associated with tungsten (left) and sulfur (right).

Raman spectra (Fig. 7) were collected using 532 nm excitation and show the two main peaks at 352 and 419 cm^{-1}, assigned to the E_{1g} and A_{1g} vibrational modes of WS_2, respectively; the weaker features present in the Raman spectra are also consistent with literature data for WS_2.[30]

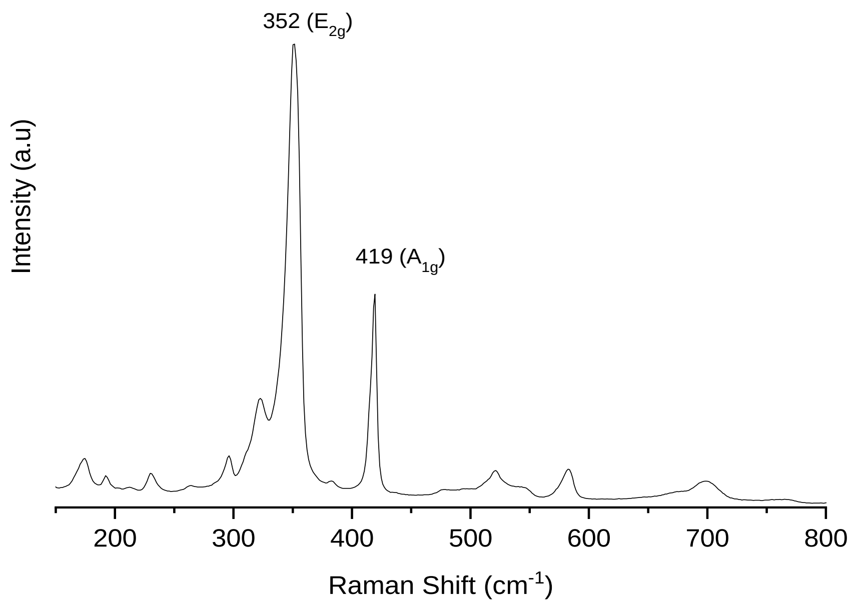

Figure 7 Raman spectrum of the WS_2 film obtained using [$(WSCl_4)_2${$^iPrS(CH_2)_2S^iPr$}]

The WS_2 thin film deposition, which constitutes the first successful low pressure CVD growth of WS_2 from a single source precursor, is very encouraging, especially given the relatively high molecular weight of the precursor and its inherently low stability (containing a soft thioether ligand bound to a hard, high oxidation state W(VI) Lewis acid). It is likely that the dinuclear precursor decomposes to a more volatile species on heating *in vacuo,* but decomposition to the W(V) analogue, [$WSCl_3${$^iPrS(CH_2)_2S^iPr$}], does not appear to be involved, since the pre-formed [$WSCl_3${$^iPrS(CH_2)_2S^iPr$}] complex does not afford WS_2 films by low pressure CVD under similar conditions. The Raman, SEM, XPS and XRD data show that the deposited WS_2 films are of good quality. However, we note that the temperature range for the deposition is rather limited, and coupled with the incomplete precursor evaporation during the CVD experiment, suggests that this dinuclear species may not be the ideal precursor. While the thiochloride-based single source CVD precursor development for WS_2 (and NbS_2 [6]) films incorporates rational design features, the complexes behave quite differently from the Ta(V) analogue,[7] indicating that not all of the factors necessary for the development of effective CVD precursors are understood and so success is still a mixture of trial, error and to some extent, serendipity. Work is currently underway to further improve the WS_2 precursor chemistry and to optimise the deposition conditions.

Conclusions

A rare series of dithioether complexes of tungsten(VI), [$(WSCl_4)_2$(dithioether)], has been synthesised and characterised both spectroscopically and by X-ray crystallography. Complexes of $WSCl_3$ have been similarly characterised, along with some dithioether complexes of $WOCl_4$ and $WOCl_3$. This work suggests that the thioether complexes of $WOCl_4$ are somewhat less stable than those of $WSCl_4$, possibly attributable to a greater hard/soft donor/acceptor mismatch in the oxide chloride system.

The first identification of a single source precursor for the production of thin films of the technologically-important[11] WS_2 by LPCVD is particularly notable, providing a potentially viable route to the growth of thin films of this important semiconducting material if satisfactory optimisation of reagents and conditions can be achieved.

Acknowledgements

We thank the EPSRC for support via EP/P025137/1 and for studentships to F.R. and D.E.S. (EP/N509747/1). We also thank Deregallera Ltd. for support (to F.R.).

Conflicts of Interest

The authors have no conflicts to declare.

Electronic Supplementary Information (ESI) includes crystallographic parameters (Table S1), crystal structures and selected bond length and angle data for $[(WSCl_4)_2\{MeS(CH_2)_2SMe\}]$ (Figs. S1). Cif files for the seven crystal structures are available from the Cambridge Crystallographic Data Centre and have been allocated CCDC numbers 1949960: $[(WSCl_4)_2\{MeS(CH_2)_3SMe\}]$, 1949963: $[(WSCl_4)_2\{MeS(CH_2)_2SMe\}]$, 1949961: $[(WSCl_4)_2\{PhS(CH_2)_2SPh\}]$, 1949964: $[(WSCl_4)_2\{^iPrS(CH_2)_3S^iPr\}]$, 1949965: $[WSCl_3\{MeS(CH_2)_2SMe\}]$, 1949962: $[WOCl_3\{MeS(CH_2)_2SMe\}]$, 1949966: $[WOCl_3\{MeS(CH_2)_3SMe\}]$. ESI also contains IR and NMR spectra for the new complexes.

References

1. G. Wilkinson, R. D. Gillard and J. A. McCleverty, *Comprehensive Coordination Chemistry*, vol 3, Pergamon, Oxford (1987).

2. D. A. Rice, *Coord. Chem. Rev*., 1978, **25**, 199.

3. R. A. Walton, *Progr. Inorg. Chem,* 1972, **16**, 1.

4. a) J. Nieboer, W. Hillary, X. Yu, H. P. A. Mercier and M. Gerken, *Inorg. Chem*., 2009, **48,** 11251; b) J. Nieboer, X. Yu, P. Chaudhary, H. P. A. Mercier and M. Gerken, *Z. Anorg. Allg. Chem*., 2012, **638**, 520.

5. a) W. Levason, G. Reid and W. Zhang, *J. Fluorine Chem.*, 2016, **184**, 50; b) J. W. Emsley, W. Levason, G. Reid, W. Zhang and G. De Luca, *J. Fluorine Chem*., 2017, **197**, 74.

6. Y.-P. Chang, A. L. Hector, W. Levason and G. Reid, *Dalton Trans.,* 2017, **46**, 9824.

7. R. D. Bannister, W. Levason, G. Reid and F. Robinson, *Polyhedron,* 2019, **169,** 129.

8. V. K. Greenacre, A. L. Hector, W. Levason, G. Reid, D. E. Smith and L. Sutcliffe, *Polyhedron*, 2019, **162,** 14.

9. W. Levason, G. Reid, D. E. Smith and W. Zhang, *Polyhedron*, in press, doi: 10.1016/j.poly.2020.114372).

10. a) M. Chhowalla, Z. Liu and H. Zhang, (Eds. - themed issue on metal dichalcogenides) C*hem. Soc. Rev.*, 2015, **44**, 2584; b) J. R. Brent, N. Savjani and P. O'Brien, Progr. Mat. Sci .2017, **89**, 411.

11 a) M. Chhowalla, H. S. Shin, G. Eda, L.-J. Li, K. P. Loh and H. Zhang*, Nat. Chem*., 2013, **5**, 263; b) J. Liu and X.-W. Liu, *Adv. Mater.,* 2012, **24**, 4097; c) K. Xu, P. Chen, X. Li, C. Wu, Y. Guo, J. Zhao, X. Wu and Y. Xie, *Angew. Chem., Int. Ed*. 2013, **52** 10477; d) H. Li, G. Lu, Y. Wang, Z. Yin, C. Cong, Q. He, L. Wang, F. Ding, T. Yu and H. Zhang, *Small*, 2013, **9**, 197.

12. a) Q. Xiang, J. Yu and M. Jaroniec, *J. Am. Chem. Soc.,* 2012, **134**, 6575; b) J. Pu, Y. Yomogida, K.-K. Liu, L.-J. Li, Y. Iwasa and T. Takenobu, *Nano Lett.,* 2012, **12**, 4013; c) Y. Ma, Y. Dsi, M. Guo, C. Niu, Y. Zhu and B. Huang, *ACS Nano*, 2012, **6**, 1695; d) K. Lee, R. Gatensby, N. McEvoy, T. Hallam and G. S. Duesberg, *Adv. Mater.,* 2013, **25**, 6699.

13. A. C. Jones and M. L. Hitchman, in *Chemical Vapour Deposition: Precursors, Processes and Applications*, ed. A. C. Jones and M. L. Hitchman, The Royal Society of Chemistry, 2009.

14. a) P. J. McKarns, T. S. Lewkebandara, G. P. A. Yap, L. M. Liable-Sands, A. L. Rheingold and C. H. Winter, *Inorg. Chem.*, 1998, **37**, 418; b) S. D. Reid, A. L. Hector, W. Levason, G. Reid, B. J. Waller and M. Webster, *Dalton Trans.*, 2007, 4769; c) S. L. Benjamin, C. H. de Groot, C. Gurnani, A. L. Hector, R. Huang, K. Ignatyev, W. Levason, S. J. Pearce, F. Thomas and G. Reid, *Chem. Mater.*, 2013, **25**, 4719; d) N. D. Boscher, C. J. Carmalt and I. P. Parkin, *Chem. Vap. Deposition*, 2006, **12**, 54; e) N. D. Boscher, C. J. Carmalt and I. P. Parkin, *Eur. J. Inorg. Chem.*, 2006, 1255; f) S. L. Benjamin, Y.-P. Chang, C. Gurnani, A. L. Hector, M. Huggon, W. Levason and G. Reid, *Dalton Trans.,* 2014, **43**, 16640.

15. a) N. E. Richey, C. Haines, J. L. Tarni and L. McElwee-White, *Chem. Commun.,* 2017, **53**, 7728; b) A. A. Tedstone, E. A. Lewis, N. Savjani, X. L. Zhong, S. H. Haigh, P. O'Brien and D. J. Lewis, *Chem. Mater.,* 2017, **29**, 3858.

16. a) X. Duan, C. Wang, A. Pan, R. Yu and X. Duan, *Chem. Soc. Rev.,* 2015, **44**, 8859; b) J. Quingqing, Yu. Zhang, Y. Zhang and Z. Liu, *Chem. Soc. Rev.,* 2015, **44,** 2587; c) C. J. Carmalt,

I. P. Parkin and E. S. Peters, *Polyhedron*, 2003, **22**, 1499; d) B. Groven, D. Claes, M. A. Nalin, H. Bender, W. Vandervorst, M. Heyns, M. Caymax, I. Radu and A. Delabie, *J. Chem. Phys*., 2019, **150**, 104703.

17. D. Britnell, G. W. A. Fowles and D. A. Rice, *J. Chem. Soc., Dalton Trans.,* 1975, 213.
18. D. Britnell, M. G. B. Drew, G. W. A. Fowles and D. A. Rice, *Inorg. Nucl. Chem. Letts.* 1973, **9**, 301.
19. M. G. B. Drew, G. R. Griffin and D. A. Rice, *Inorg. Chim. Acta,* 1979, **34**, L192.
20. F. R. Hartley, S. G. Murray, W. Levason, H. E. Soutter and C. A. McAuliffe, *Inorg. Chim. Acta,* 1979, **35,** 265.
21. V. C. Gibson, T. P. Kee and A. Shaw, *Polyhedron*, 1990, **9**, 2293.
22. a) G. M. Sheldrick, *Acta Crystallogr., Sect. C,* 2015, **71**, 3; b) G. M. Sheldrick, *Acta Crystallogr., Sect. A,* 2008, **64**, 112; c) O. V. Dolomanov, L. J. Bourhis, R. J. Gildea, J. A. K. Howard and H. Puschmann, *J. Appl. Crystallogr.,* 2009, **42**, 339.
23. ICSD: Inorganic Crystal Structure Database (ICSD), Fachinformationszentrum Karlsruhe (FIZ), accessed via the EPSRC funded National Chemical Database Service hosted by the Royal Society of Chemistry.
24. P. J. Jones, W. Levason, J. S. Ogden, J. W. Turff, E. M. Page and D. A. Rice, *J. Chem. Soc., Dalton Trans*., 1983, 2625.
25. a) G. W. A. Fowles and J. L. Frost, *J. Chem. Soc. (A),* 1967, 671; b) E. A. Allen, B. J. Brisdon, D. A. Edwards, G. W. A. Fowles and R. G. Williams, *J. Chem. Soc.,* 1963, 4649.
26. T. J. Meyer and J. A. McCleverty (Eds), *Comprehensive Coordination Chemistry II*, vols **4** and **5**, Elsevier, Oxford, 2004.
27. Y.-P. Chang, A. L. Hector, W. Levason, G. Reid and J. Whittam, *Dalton Trans.,* 2018, **47**, 2406.
28. W. J. Schutte, J. L.de Boer and F. Jellinek, *J. Solid State Chem*., 1987, **70,** 207.
29. a) J. Huang, X. Wang, J. Li, L. Cao, Z. Xu and H. Wei, *J. Alloys Compds*, 2016, **673**, 60e66; b) D. J. Morgan, *Surf. Sci. Spectra*, 2018, **25**, 014002-1.
30. a) A. Berkdemir, H. R. Gutierrez, A. R. Botello-Mendez, N. Perea-Lopez, A. L. Elıas, C. Chia, B. Wang, V. H. Crespi, F. Lopez-Urıas, J.-C. Charlier, H. Terrones and M Terrones, *Sci. Rep*., 2013, **3**, 1755; b) A. A. Mitioglu, P. Plochocka, G. Deligeorgis, S. Anghel, L. Kulyuk, and D. K. Maude, *Phys. Rev. B,* 2014, **89**, 245442; c) M. Thripuranthaka, R. V. Kashid, C. S. Rout and

D. J. Late, App. Phys. Lett., 2014, 104, 081911, d) M. R. Molas, K. Nogajewski, M. Potemski and A. Babiński, *Sci. Rep.*, 2017, **7**, 5036.